

COLOR IMAGE ENHANCEMENT USING SINGLE-SCALE RETINEX BASED ON AN IMPROVED IMAGE FORMATION MODEL

Doo Hyun Choi¹, Ick Hoon Jang², Mi Hye Kim³, and Nam Chul Kim³

1: Research Institute, Medison Co. Ltd.

1003 Daechidong, Gangnamgu, 135-280, Seoul, Korea

phone: + (82) 2 2194 1249, fax: + (82) 2 2194 1399, email: doohyunchoi@medison.com

2: Dept. of Electronic Engineering, Kyungwoon University

55 Induk, Sandongmyun, 730-850, Gumi, Korea

phone: + (82) 54 479 1213, fax: + (82) 54 479 1029, email: ihjang@ikw.ac.kr

3: Dept. of Electronic Engineering, Kyungpook National University

1370 Sankyukdong, Bukgu, 702-701, Daegu, Korea

phone: + (82) 53 950 5530, fax: + (82) 53 950 5505, email: nckim@ee.knu.ac.kr

web: vcl.knu.ac.kr

ABSTRACT

In this paper, we present an improved image formation model and propose a color image enhancement using single-scale retinex based on the model. In the presented image formation model, an input image is represented as the product of global illumination, local illumination, and reflectance. In the proposed color image enhancement, an input RGB color image is converted into an HSV color image. Under the assumption of white-light illumination, the H and S component images remain as they are and only the V component image is enhanced based on the improved image formation model. In the enhancement of V component image, the global illumination is estimated by applying a linear LPF with wide support region and the local illumination by applying a JND (just noticeable difference)-based nonlinear LPF with narrow support region. The reflectance is estimated by dividing the input V component image by the estimated global and local illuminations. After performing the gamma correction on the three estimated components, the enhanced output V component image is obtained from the product of the three results. Finally an output RGB color image is obtained from the original H and S component images and the output V component image. Experimental results show that the proposed method gives output color images of well-increased global and local contrasts, of no color change, and of nearly halo artifact free so that it yields better performance over the conventional color image enhancement methods.

1. INTRODUCTION

In recent days, as camera-equipped portable digital terminals are popularized, people have many chances to acquire images extemporaneously in the open air. However, such a situation may give an image acquisition under irregular illumination so that the image may be degraded in such a way of having excessively dark or bright regions in its parts. Up to now, various techniques such as intensity transforma-

tion [1], [2], histogram modeling [3], homomorphic filtering [4], and retinex [5]-[10] have been proposed to enhance images degraded by irregular illumination. These methods usually enhance an input image by reducing its dynamic range and/or increasing its contrast. Besides, an image enhancement based on a model of retinal processing is found in [11].

The intensity transformation converts the intensity levels of an input image using a specific transformation function such as linear function, logarithmic function, or power function [1], [2]. The case of intensity transformation using linear function is called contrast stretching or gain/offset correction and that using power function gamma correction. The histogram modeling enhances an input image by modifying its histogram as a desired shape [3]. The histogram modeling in which the desired shape of histogram is uniform is called histogram equalization. The histogram equalization is the most widely used technique in histogram modeling.

The homomorphic filtering [4] is an image enhancement method based on the image formation model that represents an input image as the product of the illumination and the reflectance. The retinex [5]-[10] is another image formation model-based enhancement. In retinex, one or both of the illumination and the reflectance is first estimated, the estimated terms are next enhanced, and the output image is finally obtained by combining the enhanced terms.

In Jobson *et al.*'s retinex [5], the illumination is first estimated by applying a Gaussian-form linear LPF to an input image. The log signal of the reflectance is then estimated by subtracting the log signal of the estimated illumination from the log signal of the input image. The estimated reflectance in log domain is used as an output image. Finally a canonical gain/offset correction is applied to adjust the brightness range of the output image to that of the output device.

In Jobson *et al.*'s retinex, the halo artifact may occur [6]-[8] that wide spreading of abrupt edges in the estimated illumination and in turn overshoots near the edges in the

output image. If the support region of the used linear LPF is narrow (wide), the estimated illumination smooths in small (large) regions so that it may give an output image in which the halo artifact occurs in small (large) regions near edges and the local (global) contrast increases.

Thereafter some efforts to reduce the halo artifact have been performed. Jobson *et al.* [9] proposed another retinex that gives an output image as the weighted sum of the retinex output images by using several linear LPFs having different support regions. This method is called multi-scale retinex (MSR) and the retinex with a linear LPF proposed in [5] single-scale retinex (SSR) [9]. Kimmel *et al.* proposed an SSR that adopts quadratic programming [6], Ogata *et al.* an MSR using an ϵ -filter [7], Choi *et al.* an SSR using a JND-based nonlinear filter [8], and Meylan and Süssstrunk an SSR using an adaptive filter [10].

In RGB color image enhancement, image enhancement methods are usually applied to each R, G, B component image independently. In Jobson *et al.*'s SSR [5] and MSR [9], the SSR and MSR are independently applied to each R, G, B component image of an RGB color image. In these methods, the component ratio of RGB at each pixel may be changed since each R, G, B component image is enhanced independently. So color change in the output image may occur. They may also give color shift to gray, called as gray-world violation, if the estimated reflectances of RGB component images have similar values [5], [6], [8], [9]. In order to make up for the problems, a multi-scale retinex with color restoration (MSRCR) was proposed [9].

In [6], the authors applied their image enhancement method to each R, G, B component image of RGB color images. They also tried to enhance RGB color images by transforming input RGB color images into HSV color images and enhancing only the V component image. The enhanced RGB color image is finally obtained by transforming the enhanced V component image along with the original H and S component images into RGB color images. In [8], an input RGB color image is transformed into HSV color image and the S and V component images are enhanced. In [10], an input RGB color image is transformed into luminance and chrominance component images by using a principal component analysis and only the luminance component image is then enhanced.

In this paper, we first present an image formation model improved from the conventional one and then propose a color image enhancement using SSR based on the model. In the presented image formation model, an input image is represented as the product of global illumination, local illumination, and reflectance to facilitate simultaneous increasing of the global and local contrasts. In the proposed color image enhancement, an input RGB color image is converted into an HSV color image. Under the assumption of white-light illumination, the H and S component images remain as they are and the V component image only is enhanced based on the improved image formation model to prevent the color change. The local illumination is estimated by applying a JND-based nonlinear filter with narrow support region to restrain the halo artifact.

2. COLOR IMAGE ENHANCEMENT USING JOBSON ET AL'S RETINEX

2.1 Conventional Image Formation Model

In the conventional image formation model, a color component image $f_i(x, y)$, $i \in \{R, G, B\}$ of an RGB color image is represented as follows [1], [4], [5]:

$$f_i(x, y) = l_i(x, y) r_i(x, y), \quad i \in \{R, G, B\} \quad (1)$$

where $l_i(x, y)$ and $r_i(x, y)$ denote the color components of the illumination and the reflectance, respectively. The illumination $l_i(x, y)$ (reflectance $r_i(x, y)$) is usually assumed to vary slowly (rapidly) so that its frequency spectrum is assumed to be mainly distributed in low (high) frequency band. Based on (1), an image formation model-based image enhancement can be applied to the color component images of an input RGB color image.

2.2 Jobson Et Al's Retinex

In Jobson *et al.*'s SSR, the illumination $l_i(x, y)$ is first estimated by applying a Gaussian-form linear LPF to an input color image $f_i(x, y)$, the output color image $\hat{f}_i(x, y)$ is then obtained by subtracting the log signal of the estimated illumination $\log \hat{l}_i(x, y)$ from the log signal of input color image $\log f_i(x, y)$ as follows [5]:

$$\hat{f}_i(x, y) = \log f_i(x, y) - \log \hat{l}_i(x, y), \quad i \in \{R, G, B\}. \quad (2)$$

In Jobson *et al.*'s MSR, the output color image $\hat{f}_{MSR_i}(x, y)$, $i \in \{R, G, B\}$ is obtained as the weighted sum of the several SSR output color images using Gaussian-form linear LPFs having different support regions as follows [9]:

$$\hat{f}_{MSR_i}(x, y) = \sum_{n=1}^N w_n \hat{f}_{n_i}(x, y), \quad i \in \{R, G, B\} \quad (3)$$

where N denotes the number of scales, $\hat{f}_{n_i}(x, y)$ the SSR output color image with the n th scale LPF, and w_n a weighting factor for the $\hat{f}_{n_i}(x, y)$.

In Jobson *et al.*'s MSRCR, the color restoration is added to the MSR as follows [9]:

$$\hat{f}_{MSRCR_i}(x, y) = C_i(x, y) \hat{f}_{MSR_i}(x, y), \quad i \in \{R, G, B\} \quad (4)$$

where $\hat{f}_{MSRCR_i}(x, y)$ denotes the MSRCR output color image. The $C_i(x, y)$ in (4) denotes a weighting function for the color restoration represented as

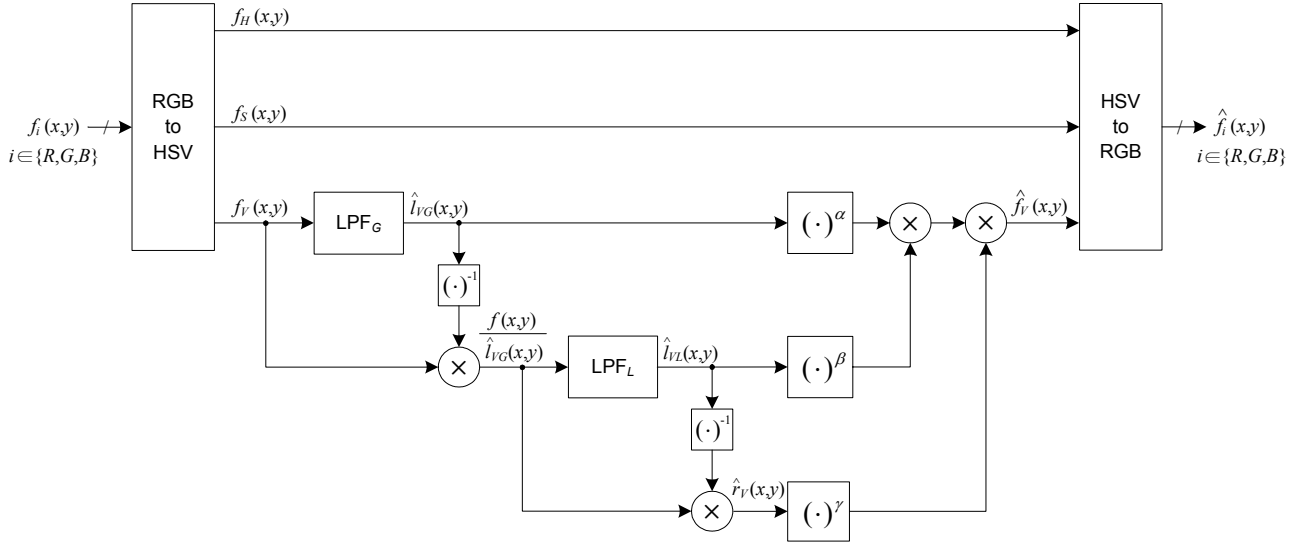


Fig. 1. Block diagram of the proposed color image enhancement.

$$C_i(x, y) = b \log \left[a \frac{f_{MSR_i}(x, y)}{\sum_{j \in \{R, G, B\}} f_{MSR_j}(x, y)} \right], \quad i \in \{R, G, B\} \quad (5)$$

where a and b denote constants.

The final SSR, MSR, or MSRCR output color image is obtained by applying the canonical gain/offset correction [5], [9] to the SSR, MSR, or MSRCR output color image to adjust its brightness range to that of the output device.

2.3 Color Image Enhancement in HSV Color Space

If we assume that the illumination is white-light, then its values of R, G, and B color components become the same, that is the illumination component $l_i(x, y)$, $i \in \{R, G, B\}$ becomes the same value $l(x, y)$. In this case, (1) can be represented as

$$f_i(x, y) = l(x, y) r_i(x, y), \quad i \in \{R, G, B\}. \quad (6)$$

Using the color transformation of RGB into HSV [12], it can be easily shown that RGB color component images $f_i(x, y)$, $i \in \{R, G, B\}$ given as (6) can be transformed into HSV color component images $f_j(x, y)$, $j \in \{H, S, V\}$ which have the relations of

$$f_H(x, y) = r_H(x, y) \quad (7)$$

$$f_S(x, y) = r_S(x, y) \quad (8)$$

$$f_V(x, y) = l(x, y) r_V(x, y) \quad (9)$$

where $r_j(x, y)$, $j \in \{H, S, V\}$ denote the color components of the reflectance transformed from $r_i(x, y)$, $i \in \{R, G, B\}$. From (7)-(9), one can see that the H and S chrominance

component images are irrelevant with the illumination and the V component image is dependent only on the illumination. Accordingly, enhancing only the V component image and converting the result HSV color image into an RGB color image, we can obtain an output color image in which the effect of the illumination is complemented without color change.

3. PROPOSED COLOR IMAGE ENHANCEMENT

Fig. 1 shows the block diagram of the proposed color image enhancement.

3.1. Improved Image Formation Model

Let us remember that in the image formation model (1), an image is represented as the product of the illumination and the reflectance. However, in real-world images, it is not often solved only with illumination and reflection under global light sources, but additionally with local light sources and shadows and their interaction. We thus suppose such a complex illumination is resolved into global illumination and local illumination. The former corresponds to the illumination that varies very slowly in an entire image, but the latter reflects local states not described by the former. The latter is assumed to vary more rapidly than the former but more slowly than the reflectance. As a result, our improved image formation model for V component image is written as

$$f_V(x, y) = l_{VG}(x, y) l_{VL}(x, y) r_V(x, y) \quad (10)$$

where $l_{VG}(x, y)$ and $l_{VL}(x, y)$ denote the global illumination and the local illumination, respectively, and $r_V(x, y)$ the reflectance.

3.2. Estimation of Global Illumination

The global illumination $l_{VG}(x, y)$ is estimated by applying a linear LPF having wide support region to the $f_V(x, y)$ as follows:

$$\begin{aligned}\hat{l}_{VG}(x, y) &= \text{LPF}_G[f_V(x, y)] \\ &= \sum_{(m, n) \in W_2} f_V(x - m, y - n) h(m, n)\end{aligned}\quad (11)$$

where $h(m, n)$ denotes the impulse response of the linear LPF and W_2 the two-dimensional (2-D) filter window. In this paper, in order to lower the computational complexity of the filtering, we adopt Gaussian pyramid filtering [13] which performs iteratively while widening the support region of the filter. In each iteration, we also apply a 1-D linear LPF to the horizontal and vertical signals in separable fashion.

3.3. Estimation of Local Illumination and Reflectance

For the estimation of local illumination $l_{VL}(x, y)$, a nonlinear LPF with narrow support region is applied to the image $f_{V1}(x, y)$ in which the estimated global illumination $\hat{l}_{VG}(x, y)$ is eliminated from the $f_V(x, y)$, that is $f_{V1}(x, y) = f_V(x, y) / \hat{l}_{VG}(x, y)$ as follows:

$$\begin{aligned}\hat{l}_{VL}(x, y) &= \text{LPF}_L[f_{V1}(x, y)] \\ &= \frac{1}{\Lambda(x, y)} \sum_{(m, n) \in W_2} f_{V1}(x - m, y - n) h(m, n) \lambda(x, y; m, n)\end{aligned}\quad (12)$$

$$\Lambda(x, y) = \sum_{(m, n) \in W_2} h(m, n) \lambda(x, y; m, n)\quad (13)$$

where $\lambda(x, y; m, n)$ denotes a weighting function for the adjustment of the filter coefficients so that the filtering in (12) is the JND-based nonlinear LPF filtering proposed in [8], which was shown to restrain the halo artifact in enhanced images. We also adopt Gaussian pyramid filtering as in the case of the estimation of global illumination.

The reflectance is estimated by eliminating the $\hat{l}_{VG}(x, y)$ and the $\hat{l}_{VL}(x, y)$ from the $f_V(x, y)$ as follows:

$$\hat{r}_V(x, y) = \frac{f_V(x, y)}{\hat{l}_{VG}(x, y) \hat{l}_{VL}(x, y)}.\quad (14)$$

3.4. Color Image Enhancement

In the enhancement of the V component image, the estimated global illumination, local illumination, and reflectance are enhanced by applying gamma corrections, and the output V component image $\hat{f}_V(x, y)$ is obtained as the product of the three results as

$$\hat{f}_V(x, y) = (\hat{l}_{VG}(x, y))^\alpha (\hat{l}_{VL}(x, y))^\beta (\hat{r}_V(x, y))^\gamma\quad (15)$$

where α , β , and γ denote gamma factors. These have the relation of $0 \leq \alpha \leq \beta \leq \gamma$ considering the fact that the low



Fig. 2. An input color image 1 and the result images. (a) Input image, (b) MSRCR, (c) Meylan and Süssstrunk, and (d) proposed method.

frequency band has more important effect on the dynamic range compared to the high frequency band. They may be further determined considering the taste of a user on the contrast, brightness, and naturalness of the output color image.

Finally, the enhanced RGB color image is obtained by transforming the final output V component image along with the original H and S component images.

4. EXPERIMENTAL RESULTS AND DISCUSSION

To evaluate the performance of the proposed color image enhancement, we used eight test color images of 2000×1312 size downloaded from the home page of TruView Imaging Company [14] and two of 1155×859 from IVRG [15]. We compared the performance of the proposed method with those of the MSRCR [9] and Meylan and Süssstrunk's method [10]. The iteration numbers of the linear and JND-based nonlinear LPF filterings were chosen as 9 and 5, respectively, the 1-D filter coefficients as $h(m) = h(n) = [0.25, 0.5, 0.25]$, for $m, n = -1, 0, 1$, and the gamma factors α , β , and γ as 0.2, 0.4, and 0.8, respectively. The parameters for the JND were also chosen as in [8].

Fig. 2 shows that an input color image 1, where there are strong edges in the center part and weak edges in the left and right parts, and the result images by the MSRCR, Meylan and Süssstrunk's method, and the proposed method. In the MSRCR output image of Fig. 2(b), one can see that the global and local contrasts increase well. However, the trees in the lower left part are still dark. In the output image of Meylan and Süssstrunk's method in Fig. 2(c), we can see that the global and local contrasts also increase well without the halo artifact. However, it is rather globally brighter compared to the other images. One can see from the output image of the proposed method in Fig. 2(d) that the local contrasts of the tower and the white wall increase well compared to those of the Meylan and Süssstrunk's method. In addition, it does not yield the color change and is nearly free of the halo artifact and the over-enhancement.

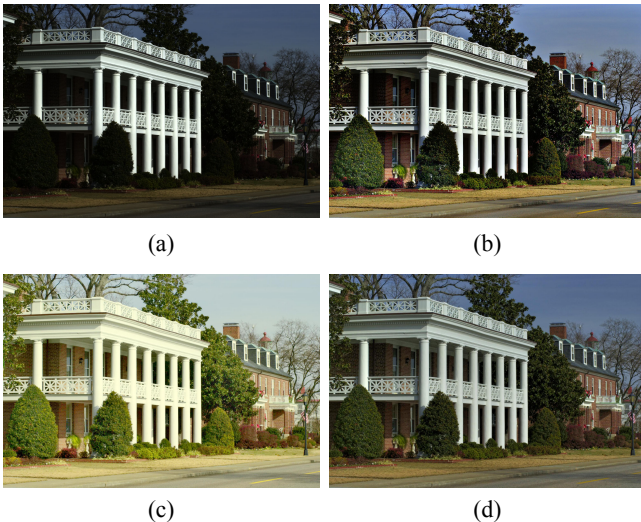


Fig. 3. An input color image 2 and the result images. (a) Input image, (b) MSRCR, (c) Meylan and Süssstrunk, and (d) proposed method.

Fig. 3 shows an input color image 2, where there are white and bright pillars having strong edges and dark trees having weak edges, and the result images by the three methods. In the MSRCR output image of Fig. 3(b), one can see that the walls between the pillars are still dark. In Fig. 3(c) of Meylan and Süssstrunk's method, we can see that the global and local contrasts increase well without such regions. However, the color of the leaves of trees is changed to yellow-green. In Fig. 3(d) of the proposed method, one can see that the local and global contrasts increase well without the color change.

Fig. 4 shows an input color image 3, where there are a big tree having strong and weak edges and woods and clouds having weak edges, and the result images by the three methods. In Fig. 4(b) of the MSRCR output image, one can see that some leaves of the big tree are still dark. From the output image of Meylan and Süssstrunk's method in Fig. 4(c), we can see that the local contrasts near the clouds increase rather excessively. On the contrary, in Fig. 4(d) of the proposed method, one can see that the local and global contrasts increase well without such regions.

Experimental results for the other test color images have shown similar tendencies to the three test images. We can see from these results that the proposed method increases the global and local contrasts simultaneously well due to the basis on the improved image formation model, does not yield the color change due to enhancing only the V component image, and nearly restrains the halo artifact due to the adoption of JND-based nonlinear LPF.

REFERENCES

- [1] R. C. Gonzalez and R. E. Woods, *Digital Image Processing*. Reading, MA: Addison-Wesley, 1992.
- [2] W. K. Pratt, *Digital Image Processing*, 2nd ed. New York: Wiley, 1991.
- [3] A. K. Jain, *Fundamentals of Digital Image Processing*. Englewood Cliffs, NJ: Prentice-Hall, 1989.

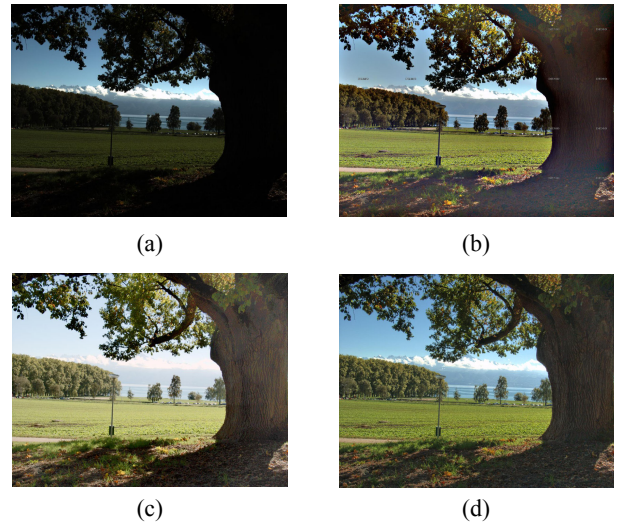


Fig. 4. An input color image 3 and the result images. (a) Input image, (b) MSRCR, (c) Meylan and Süssstrunk, and (d) proposed method.

- [4] J. S. Lim, *Two-Dimensional Signal and Image Processing*. Englewood Cliffs, NJ: Prentice-Hall, 1990.
- [5] D. J. Jobson, Z. Rahman, and G. A. Woodell, "Properties and performance of a center/surround retinex," *IEEE Trans. Image Process.*, vol. 6, no. 3, pp. 451–462, Mar. 1997.
- [6] R. Kimmel, M. Elad, D. Shaked, R. Keshet, and I. Sobel, "A variational framework for retinex," *Int. J. Comput. Vis.*, vol. 52, no. 1, pp. 7–23, Jan. 2003.
- [7] M. Ogata, T. Tsuchiya, T. Kubozono, and K. Ueda, "Dynamic range compression based on illumination compensation," *IEEE Trans. Consumer Electron.*, vol. 47, no. 3, pp. 548–558, Aug. 2001.
- [8] D. H. Choi, I. H. Jang, M. H. Kim, and N. C. Kim, "Color image enhancement based on single-scale retinex with a JND-based nonlinear filter," in *Proc. IEEE Int. Symp. Circuits and Syst.*, New Orleans, USA, May 2007, pp. 3948–3951.
- [9] D. J. Jobson, Z. Rahman, and G. A. Woodell, "A multi-scale retinex for bridging the gap between color images and the human observation of scenes," *IEEE Trans. Image Process.*, vol. 6, no. 7, pp. 965–976, July 1997.
- [10] L. Meylan and S. Süssstrunk, "High dynamic range image rendering with a retinex-based adaptive filter," *IEEE Trans. Image Process.*, vol. 15, no. 9, pp. 2820–2830, Sep. 2006.
- [11] L. Meylan, D. Alleysson, and S. Süssstrunk, "Model of retinal local adaptation for the tone mapping of color filter array images," *J. Opt. Soc. Am. A*, vol. 24, no. 9, pp. 2807–2816, Sep. 2007.
- [12] R. W. G. Hunt, *Measuring Color*. New York: Halsted Press, 1989.
- [13] P. J. Burt and E. H. Adelson, "The Laplacian pyramid as a compact image code," *IEEE Trans. Commun.*, vol. COM-31, no. 4, pp. 532–540, Apr. 1983.
- [14] [Online]. Available: <http://www.truview.com>
- [15] [Online]. Available: <http://ivrg.epfl.ch>